Localization and Spreading of Diseases in Complex Networks

A. V. Goltsev,[1,2] S. N. Dorogovtsev,[1,2] J. G. Oliveira,[1,3] and J. F. F. Mendes[1]

[1]*Department of Physics, I3N, University of Aveiro, 3810-193 Aveiro, Portugal*
[2]*Ioffe Physico-Technical Institute, 194021 St. Petersburg, Russia*
[3]*Departamento de Engenharia Física, Faculdade de Engenharia, Universidade do Porto,
rua Dr. Roberto Frias, 4200-465 Porto, Portugal*

Using the susceptible-infected-susceptible model on unweighted and weighted networks, we consider
the disease localization phenomenon. In contrast to the well-recognized point of view that diseases infect a
finite fraction of vertices right above the epidemic threshold, we show that diseases can be localized on a
finite number of vertices, where hubs and edges with large weights are centers of localization. Our results
follow from the analysis of standard models of networks and empirical data for real-world networks.

A survey of infectious diseases reveals that before an
outbreak, often, if not typically, a disease is localized
within a small group of individuals. Changes in environ-
mental conditions or increase in the frequency of external
contacts result in an epidemic outbreak. In this Letter,
we propose an approach that enables us to describe
quantitatively this important localization-delocalization
phenomenon. Our approach is based on the susceptible-
infected-susceptible (SIS) model [1,2] of spreading of
diseases in weighted and unweighted networks, where
the weights of edges encode frequency of contacts between
vertices. It is widely accepted that in uncorrelated
networks, the epidemic threshold λ_c of the infection rate
λ is $\lambda_{MF} = \langle q \rangle / \langle q^2 \rangle$, where $\langle q \rangle$ and $\langle q^2 \rangle$ are the first and
second moments of the degree distribution [2]. So in net-
works with a finite $\langle q^2 \rangle$, the threshold should be nonzero,
while it is zero if $\langle q^2 \rangle$ diverges. One should stress, however,
that all these well-known results were obtained only
within a mean-field theory, actually within an annealed
network approximation in which a random network is
substituted for its fully connected weighted counterpart
[2]. Contrastingly, one can show exactly for an arbitrary
graph that λ_c is actually determined by the largest eigen-
value Λ_1 of the adjacency matrix A_{ij} of the graph, and
$\lambda_c = 1/\Lambda_1 < \lambda_{MF}$ [3–11]. For uncorrelated networks, in
particular, scale-free networks with the degree exponent
$\gamma > 2.5$, it was found that Λ_1 is determined by the maxi-
mum degree q_{max}, $\Lambda_1 \propto \sqrt{q_{max}}$ [3–5]. Then, if in the
infinite size limit, q_{max} tends to infinity, as, e.g., in the
Erdős–Rényi graphs, this leads to the amazing conclusion
that the epidemic threshold is absent even in (infinite)
networks with a finite $\langle q^2 \rangle$, in contrast to the mean-field
result. The conclusion that the epidemic threshold may be
absent even in the networks with rapidly decaying degree
distributions was confirmed in numerical simulations per-
formed in Ref. [6].

In this Letter, we develop a spectral approach to the
SIS model on complex networks. We show that the

contradiction between the mean-field approximation and
the exact result can be resolved if we take into account
localization of diseases. It turns out that, in contrast to the
mean field theory, in which a finite fraction of vertices are
infected at $\lambda > \lambda_c$, there are actually two scenarios of the
spreading of diseases. If Λ_1 corresponds to a localized
eigenstate, then, at λ right above $\lambda_c = 1/\Lambda_1$, disease is
mainly localized on a finite number of vertices; i.e., the
fraction of infected vertices is negligibly small in large
networks. With further increase of λ, the disease gradually
infects more and more vertices until it will infect a finite
fraction of vertices. In the second scenario, Λ_1 corresponds
to a delocalized state. Then already at $\lambda \Lambda_1 - 1 \ll 1$, the
disease infects a finite fraction of vertices. Analyzing net-
work models and real-world networks, we show that hubs,
edges with large weights, and other dense subgraphs can be
centers of localization.

We consider the standard SIS model of disease spread-
ing in a complex network of size N having adjacency
matrix with arbitrary entries $A_{ij} \geqq 0$. Infected vertices
become susceptible with unit rate, and each susceptible
vertex becomes infected by its infective neighbor with the
infection rate λ. Neglecting correlations between infected
and susceptible vertices, the probability $\rho_i(t)$ that vertex i
is infected at time t is described by the evolution equation

$$\frac{d\rho_i(t)}{dt} = -\rho_i(t) + \lambda[1 - \rho_i(t)] \sum_{j=1}^{N} A_{ij} \rho_j(t). \quad (1)$$

In the steady state, at $t \to \infty$, the probability $\rho_i \equiv \rho_i(\infty)$ is
determined by a nonlinear equation,

$$\rho_i = \frac{\lambda \sum_j A_{ij} \rho_j}{1 + \lambda \sum_j A_{ij} \rho_j}, \quad (2)$$

which has a nonzero solution $\rho_i > 0$ if λ is larger than the
so-called epidemic threshold λ_c. In this case, the prevalence
$\rho \equiv \sum_{i=1}^{N} \rho_i / N$ is nonzero.

Spectral approach.—To solve the SIS model, we use the spectral properties of the adjacency matrix $\hat{A}$. The eigenvalues Λ and the corresponding eigenvectors $\boldsymbol{f}$ with components f_i are solutions of the equation $\Lambda \boldsymbol{f} = \hat{A}\boldsymbol{f}$. Since the matrix $\hat{A}$ is real and symmetric, its N eigenvectors $\boldsymbol{f}(\Lambda)$ ($\Lambda_{\max} \equiv \Lambda_1 \geq \Lambda_2 \geq \dots \Lambda_N$) form a complete orthonormal basis. According to the Perron–Frobenius theorem, the largest eigenvalue Λ_1 and the corresponding principal eigenvector $\boldsymbol{f}(\Lambda_1)$ of a real non-negative symmetric matrix are non-negative [12]. The probabilities ρ_i can be written as a linear superposition,

$$\rho_i = \sum_{\Lambda} c(\Lambda) f_i(\Lambda). \tag{3}$$

The coefficients $c(\Lambda)$ are the projections of the vector $\boldsymbol{\rho}$ on $\boldsymbol{f}(\Lambda)$. Substituting Eq. (3) into Eq. (2), we obtain

$$c(\Lambda) = \lambda \sum_{\Lambda'} \Lambda' c(\Lambda') \sum_{i=1}^{N} \frac{f_i(\Lambda)f_i(\Lambda')}{1 + \lambda \sum_{\tilde{\Lambda}} \tilde{\Lambda} c(\tilde{\Lambda}) f_i(\tilde{\Lambda})}. \tag{4}$$

In order to find the epidemic threshold λ_c and $\rho(\lambda)$ near λ_c, it is enough to take into account only the principal eigenvector $\boldsymbol{f}(\Lambda_1)$ in Eqs. (3) and (4), i.e., $\rho_i \approx c(\Lambda_1)f_i(\Lambda_1)$. Solving Eq. (4), with respect to $c(\Lambda_1)$, gives $\lambda_c = 1/\Lambda_1$. At $\lambda \geq \lambda_c$ in the first order in $\tau \equiv \lambda \Lambda_1 - 1 \ll 1$, we find $\rho \approx \alpha_1 \tau$, where the coefficient α_1 is

$$\alpha_1 = \sum_{i=1}^{N} f_i(\Lambda_1) / [N \sum_{i=1}^{N} f_i^3(\Lambda_1)]. \tag{5}$$

This expression is exact if there is a gap between Λ_1 and Λ_2 (see also Ref. [13]). Thus, at $\tau \ll 1$, ρ is determined by the principal eigenvector. The contribution of other eigenvectors are of the order of τ^2. Considering the two largest eigenvalues in Eq. (4), Λ_1 and Λ_2, and their eigenvectors, we obtain $\rho(\lambda) \approx \alpha_1 \tau + \alpha_2 \tau^2$ and so on.

The usual point of view is that α_1 is of the order of $O(1)$, and so a finite fraction of vertices is infected right above λ_c. To learn if another behavior is possible, we study whether Λ_1 corresponds to a localized or delocalized state. We use the inverse participation ratio

$$\text{IPR}(\Lambda) \equiv \sum_{i=1}^{N} f_i^4(\Lambda). \tag{6}$$

If, in the limit $N \to \infty$, IPR(Λ) is of the order of $O(1)$, then the eigenvector $\boldsymbol{f}(\Lambda)$ is localized. If IPR$(\Lambda) \to 0$ then this state is delocalized. For a localized $\boldsymbol{f}(\Lambda)$, the components $f_i(\Lambda)$ are of the order of $O(1)$ only at few vertices. For a delocalized $\boldsymbol{f}(\Lambda)$, we usually have $f_i(\Lambda) \sim O(1/\sqrt{N}) \ll 1$. From Eq. (5), it follows that if the principal eigenvector $\boldsymbol{f}(\Lambda_1)$ is localized, then $\alpha_1 \sim O(1/N)$ and so $\rho \approx \alpha_1 \tau \sim O(1/N)$. In this case, above λ_c the disease is localized on a finite number $N\rho$ of vertices. If $\boldsymbol{f}(\Lambda_1)$ is delocalized, then ρ is of the order of $O(1)$, and the disease infects a finite fraction of vertices right above λ_c. These two contrasting
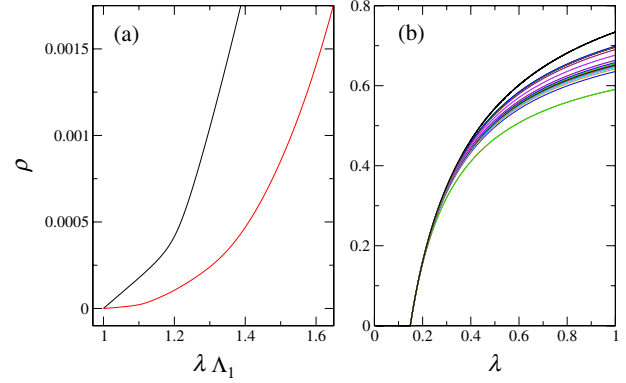

FIG. 1 (color online).   Prevalence ρ versus the infection rate λ in real networks. (a) astro-phys (upper line) and cond-mat-2005 (lower line) weighted networks [from Eq. (2)]. The eigenstate Λ_1 is localized in the cond-mat-2005 network and delocalized in the astro-phys and karate-club networks. (b) Karate-club network. The lower curve accounts for only the eigenstate Λ_1 in Eq. (4). Accounting for eigenstates Λ_1 and Λ_2, we find the higher curve and so on. The most upper curve is the exact ρ.

scenarios are shown in Fig. 1 for the SIS model on the karate-club network [14] and the weighted collaboration networks of scientists posting preprints on the astrophysics archive at arXiv.org, 1995–1999, and the condensed matter archive at January 1, 1995—March 31, 2005 [15]. The astro-ph and karate-club nets have delocalized principal eigenstates while the cond-mat-2005 net has a localized principal eigenstate. A numerical solution of Eq. (2) gives $\alpha_1 = 1.8 \times 10^{-3}$ for the astro-ph net and smaller $\alpha_1 = 1.5 \times 10^{-4}$ for the cond-mat-2005 net.

One can find Λ_1 and IPR(Λ_1) for any unweighted and weighted graph:

$$\Lambda_1 = \lim_{n \to \infty} \Lambda_1(n) \equiv \lim_{n \to \infty} (\boldsymbol{g}^{(n)} \hat{A} \boldsymbol{g}^{(n)}) / |\boldsymbol{g}^{(n)}|^2, \tag{7}$$

$$\text{IPR}(\Lambda_1) = \lim_{n \to \infty} \sum_{i=1}^{N} (g_i^{(n)})^4 / |\boldsymbol{g}^{(n)}|^4, \tag{8}$$

where $\boldsymbol{g}^{(n+1)} = \hat{A}\boldsymbol{g}^{(n)}$ and $\boldsymbol{g}^{(0)}$ is a positive vector. $\Lambda_1(n)$ is a lower bound of Λ_1. In unweighted networks, i.e., $A_{ij} = 0,1$, for $\boldsymbol{g}^{(0)} = 1$, the first iteration $n = 1$ gives

$$\Lambda_1(1) = \frac{1}{\langle q^2 \rangle N} \sum_{i,j} q_i A_{ij} q_j = \Lambda_{MF} + \frac{\langle q \rangle \sigma^2 r}{\langle q^2 \rangle}, \tag{9}$$

where $\Lambda_{MF} \equiv \langle q^2 \rangle / \langle q \rangle$, r is the Pearson coefficient, and $\sigma^2 = \langle q^3 \rangle / \langle q \rangle - \langle q^2 \rangle^2 / \langle q \rangle^2$ [16,17]. Equation (9) shows that assortative degree-degree correlations ($r > 0$) increase Λ_1 while disassortative correlations ($r < 0$) decrease Λ_1. The first iteration also gives the mean-field result IPR $= \langle q^4 \rangle / [N \langle q^2 \rangle^2] \sim O(1/N)$. A few iterations already give good approximations for Λ_1 and IPR if the principal eigenstate is delocalized but more iterations are needed if this eigenstate is localized.

Bethe lattice.—To find possible centers of localization of Λ_1, we use Bethe lattices as simple but representative examples of networks. The adjacency matrix of an unweighted regular Bethe lattice in Fig. 2(a) with vertices of degree k has the largest eigenvalue $\Lambda_1 = k$ with a delocalized eigenvector $f_i(\Lambda_1) = N^{-1/2}$. Let us introduce a hub of degree $q > k$ connected to the neighbors by edges with a weight $w \geq 1$ [see Fig. 2(b)]. The other edges have weight 1. We look for such a solution $\mathbf{f}$ of the equation $\Lambda \mathbf{f} = \hat{A}\mathbf{f}$ that has a maximum component $f_0(\Lambda_1)$ at the hub and exponentially decreases with increasing distance n from the hub, $f_i(\Lambda_1) = f_n(\Lambda_1) \propto 1/a^n$. We find

$$\Lambda_1 = qw^2/\sqrt{qw^2 - B}, \qquad (10)$$

$$\text{IPR}\,(\Lambda_1) = f_0^4(\Lambda_1)[1 + qw^4/(a^4 - B)], \qquad (11)$$

$$f_0(\Lambda_1) = [(qw^2/2 - B)/(qw^2 - B)]^{1/2}, \qquad (12)$$

$$f_n(\Lambda_1) = wf_0(\Lambda_1)/a^n. \qquad (13)$$

Here, $B \equiv k - 1$ is the branching coefficient of the graph, $a \equiv (qw^2 - B)^{1/2}$. Due to the exponential decay, IPR is finite, so this eigenstate is localized. In the limit $qw^2 \gg B$, we have IPR $\rightarrow (1 + 1/q)/4$. This solution gives the maximum eigenvalue if $\Lambda_1 > k$. This condition can be written in the form $q > q_{\text{loc}} \equiv (B^2 + B)/w^2$. The second eigenstate with $\Lambda_2 = k$ and $f_i(\Lambda_2) \approx N^{-1/2}$ is delocalized.

Now, we consider a Bethe lattice with two hubs of degrees q_1 and q_2 connected by an edge with weight $w \geq 1$ [see Fig. 2(c)]. Other edges have weight 1. As above, we look for an eigenvector $\mathbf{f}$ that exponentially decays from these hubs. We find that there are two localized eigenstates with eigenvalues Λ_1 and Λ_2 above $\Lambda_3 = k$,

$$\Lambda_{1(2)} = a_\pm + B/a_\pm,$$
$$a_\pm^2 = \frac{1}{2}(Q_1 + Q_2 + w^2) \pm \frac{1}{2}[(Q_1 + Q_2 + w^2)^2 - 4Q_1Q_2]^{1/2},$$
$$\Psi_1^2(a_\pm^2 + Q_1) + \Psi_2^2(a_\pm^2 + Q_2) = a_\pm^2 - B,$$
$$\text{IPR}(\Lambda_{1(2)}) = [\Psi_1^4(a_\pm^4 + Q_1) + \Psi_2^4(a_\pm^4 + Q_2)]/(a_\pm^4 - B).$$
$$(14)$$

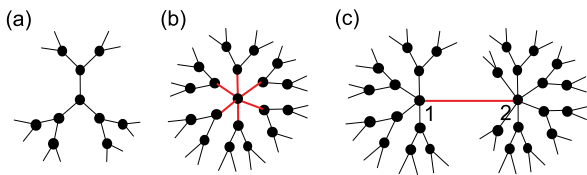

FIG. 2 (color online). (a) Regular Bethe lattice with degree $k = 3$. (b) Bethe lattice with one hub of degree $q > k$. This hub is connected to neighbors by edges having the same weight $w \geq 1$ (red or gray lines). (c) Bethe lattice with two vertices of degrees q_1 and q_2 connected by an edge with a weight $w \geq 1$ (red or gray line).

The signs $\pm$ correspond to Λ_1 and Λ_2, respectively, and $Q_{1(2)} \equiv q_{1(2)} - B - 1$. The components f_i decrease exponentially as $\Psi_{1(2)}/a_\pm^n$ with increasing distance n from the hubs 1 and 2. Ψ_1 and Ψ_2 are the components of $\mathbf{f}$ at the hubs 1 and 2. Their ratio is $\Psi_2/\Psi_1 = (a_\pm^2 - Q_1)/(wa_\pm)$. The criterion for localization is $\Lambda_1, \Lambda_2 > k$. If $q_1 = q_2$ and $w \gg 1$, then $\Psi_1 = \Psi_2 \rightarrow 1/\sqrt{2}$ and IPR(Λ_1) reaches the maximum value 0.5 that means localization on two hubs. In general, Λ_1 can be localized in a larger cluster.

Scale-free networks.—To study the appearance and properties of localized eigenstates in uncorrelated complex networks, we use the static model [18] that generates unweighted scale-free networks with degree distribution $P(q) \propto Cq^{-\gamma}$ at $q \gg 1$. Using software OCTAVE, for each realization of a random network of size N with mean degree $\langle q \rangle$ and $\gamma = 4$, we calculated eigenvalues, eigenvectors, and IPR(Λ) of the adjacency matrix. In networks of size $N = 10^5$, we found that several (typically, from one to three for different realizations) eigenstates appear above the upper delocalized eigenstate. These states are localized at hubs and their properties are described well by Eqs. (10)–(13) with $w = 1$ if the branching coefficient B in these equations is replaced by the averaged branching coefficient $B = \langle q^2 \rangle/\langle q \rangle - 1$. We observed that in these scale-free graphs, the upper delocalized eigenstate Λ_d is slightly above the mean-field value $\Lambda_{MF} = \langle q^2 \rangle/\langle q \rangle$. The maximum degree q_{max} fluctuates from realization to realization. Localization of the principal eigenstate at a vertex with degree q_{max} occurs if

$$\Lambda_1 = q_{\text{max}}/\sqrt{q_{\text{max}} - B} \gtrsim \Lambda_d. \qquad (15)$$

The equality, here, gives the threshold degree q_{loc}. In realizations with $q_{\text{max}} < q_{\text{loc}}$, the principal eigenvector is delocalized and $\Lambda_1 = \Lambda_d$. For $N = 10^5$, $\langle q \rangle = 10$, and $\gamma = 4$, our numerical calculations give $\langle q^2 \rangle/\langle q \rangle \approx 14.1$ and $\Lambda_d \approx 15$. According to Eq. (15), a localized state appears above Λ_d if q_{max} is larger than $q_{\text{loc}} \approx 214$. Since the average value of q_{max} depends on N, at small N, the probability to generate a graph with $q_{\text{max}} > q_{\text{loc}}$ is small [19]. Only large graphs can have a localized principal eigenstate. The criterion [Eq. (15)] is not satisfied at $\gamma \leq 5/2$ because Λ_d becomes larger than the eigenvalue $\Lambda \approx \sqrt{q_{\text{max}}}$ of a state localized at the vertex with q_{max}. Indeed, assuming $\Lambda_d \approx \Lambda_{MF}$, we find $\Lambda_d \propto q_{\text{max}}^{3-\gamma} > \sqrt{q_{\text{max}}}$ at $q_{\text{max}} \gg 1$ when $\gamma \leq 5/2$. Hence, the largest eigenstate is delocalized and $\Lambda_1 = \Lambda_d \approx \Lambda_{MF}$ in agreement with Refs. [4,6]. Thus, in the case of uncorrelated random graphs of sufficiently large size, the principal eigenvector is localized if $\gamma > 5/2$, which includes the Erdős–Rényi graphs, and delocalized if $2 < \gamma \leq 5/2$. Figure 3 represents the results of our numerical solution of Eq. (4) for the SIS model on one typical realization of the scale-free network. The principal eigenvector is localized at the hub with $q_{\text{max}} = 323$. Equations (10), (13), and (5) give $\Lambda_1 = 18.35$, IPR $= 0.23$, and $\alpha_1 \simeq 1.4 \times 10^{-3}$. These values agree well
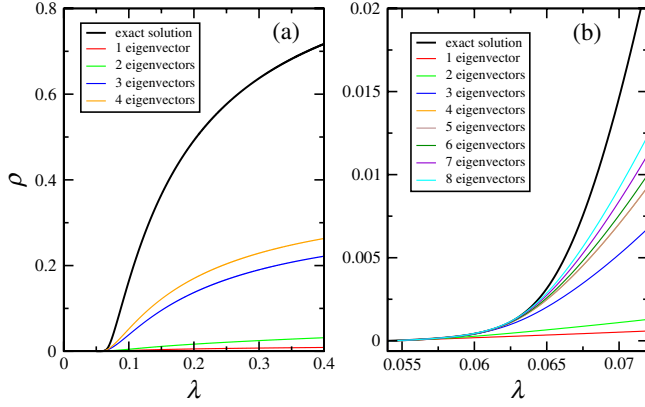
FIG. 3 (color online). (a) Prevalence ρ versus λ in a scale-free network of 10^5 vertices generated by the static model with $\gamma = 4$, $\langle q \rangle = 10$. The lowest curve accounts for only the principal eigenstate in Eq. (4), the next one accounts Λ_1 and Λ_2, and so on. (b) Zoom of the prevalence at λ near $\lambda_c = 1/\Lambda_1$.

with the measured values $\Lambda_1 = 18.47$, IPR $= 0.21$, and $\alpha_1 \simeq 1.7 \times 10^{-3}$. The eigenvector with Λ_2 is localized at the second largest hub with $q = 254$. The third eigenvector with $\Lambda_3 \approx 15.3$ is delocalized. The first two eigenstates allow us to describe $\rho(\lambda)$ close to $\lambda_c = 1/\Lambda_1$. Accounting for the delocalized eigenstate Λ_3 gives better results in a broader range of λ (see Fig. 3).

Real networks.—The largest eigenvalue Λ_1, IPR(Λ_1), and other parameters of a few weighted and unweighted real-world networks are given in Table I. Note first, that in all of these unweighted real networks the inverse participation ratio IPR(Λ_1) is small, that evidences a delocalized Λ_1. We suggest that localization does not occur because the localization threshold q_{loc} from the criterion Eq. (15) exceeds q_{max}. Second, in unweighted networks, Λ_1 differs strongly from the mean-field value $\Lambda_{MF} = \langle q^2 \rangle / \langle q \rangle$. Λ_1 is larger than Λ_{MF} in networks with assortative mixing (cond-mat 2005, hep-th, and astro-ph networks) while Λ_1 is smaller than Λ_{MF} in disassortative networks (karate-club network). Qualitatively, this agrees with Eq. (9). A similar observation was made in Refs. [9,11]. Table I shows that

in contrast to the unweighted hep-th and cond-mat-2005 networks, their weighted versions have a localized principal eigenvector with a large IPR. Localization occurs at vertices linked by edges with a large weight. In the cond-mat-2005 network, localization occurs at two vertices of degrees 37 and 28 connected by an edge with weight 34.3 that is much larger than the average weight $\overline{w} = 0.51$. In this case, Eq. (14) gives $\Lambda_1 \approx 34.5$ and IPR ≈ 0.49. In the hep-th network, the strong edge has weight 34 larger than $\overline{w} = 0.97$ and connects two vertices of degrees 34 and 33. Using Eq. (14), we find $\Lambda_1 \approx 35$ and IPR ≈ 0.47 in agreement with the data in Table I. The components of the principal eigenvectors in these networks decay exponentially with distance from the strong edges in agreement with Eq. (14). In the astro-ph weighted network, none of the edges satisfies the localization criterion. Two scenarios of behavior of the prevalence $\rho(\lambda)$ in weighted networks with localized and delocalized Λ_1 are shown in Fig. 1(a). Although above we considered only localization centers with one or two vertices, note that a disease may also be localized on larger finite clusters.

It was concluded in Refs. [9,11] that in unweighted networks a disease first survives inside the higher k-cores. By definition, k-cores are subgraphs containing a finite fraction of a network, and so these two works actually discussed the delocalized state of disease. The principal difference of the present work from Refs. [9,11] is that we consider situations in which a disease takes in a finite number of vertices and not a finite fraction both in unweighted and weighted networks.

In conclusion, based on a spectral approach to the SIS model, we showed that if the principal eigenvector of the adjacency matrix of a network is localized, then at the infection rate λ right above the threshold $1/\Lambda_1$, the disease is mainly localized on a finite number of vertices. Importantly, a strict epidemic threshold in this case is actually absent, and a real epidemic affecting a finite fraction of vertices occurs after a smooth crossover, at higher values of λ. On the other hand, if the principal eigenvector is delocalized, the epidemic occurs in the whole region above $\lambda_c = 1/\Lambda_1$. We suggest that further investigations of

TABLE I. Characteristics of real-world networks. N is size, γ is the degree distribution exponent, q_{max} is the maximum degree, q_{loc} is the localization threshold found from Eq. (15), Λ_1 is the largest eigenvalue, and $\Lambda_1(1)$ is its lower bound, Eq. (9), respectively. A and D stand for assortative and disassortative mixing. Two last columns represent weighted networks.

Network	N	γ	q_{max}	q_{loc}	$\langle q^2 \rangle / \langle q \rangle$	mixing	Λ_1	$\Lambda_1(1)$	IPR(Λ_1)	Λ_1 weighted	IPR(Λ_1) weighted
cond-mat 2005 [15]	40421	3.0	278	2604	27.35	A	51.29	35.205	0.0081	47.63	0.3415
hep-th [15]	8361		50	521	8.687	A	23	10.632	0.0417	40.52	0.3531
astro-ph [15]	16706		360	5415	44.92	A	73.89	56.287	0.005	33.7575	0.0525
power grid [20]	4941	exponential	19	53	3.87		7.483	3.9	0.041		
fp5 [21]	27985	2.2	2942	38610	211.0		197.03	176.3	0.0035		
CAIDA (router-internet) [22]	192244	2.7	1071	11947	37.89		109.5	42.9	0.010		
karate-club [14]	34		17	37	7.77	D	6.72	6.01	0.073		

real-world networks will give many new examples of disease localization-delocalization phenomena.

[1] R. Albert and A.-L. Barabási, Rev. Mod. Phys. **74,** 47 (2002); S. N. Dorogovtsev and J. F. F. Mendes, Adv. Phys. **51,** 1079 (2002); M. E. J. Newman, SIAM Rev. **45,** 167 (2003); S. N. Dorogovtsev, A. V. Goltsev, and J. F. F. Mendes, Rev. Mod. Phys. **80,** 1275 (2008).

[2] R. Pastor-Satorras and A. Vespignani, Phys. Rev. Lett. **86,** 3200 (2001); Phys. Rev. E **63,** 066117 (2001); M. Boguñá, R. Pastor-Satorras, and A. Vespignani, Phys. Rev. Lett. **90,** 028701 (2003).

[3] Y. Wang, D. Chakrabarti, C. Wang, and C. Faloutsos, in *22nd International Symposium on Reliable Distribute Systems (SRDS03)* (IEEE Computer Society, Los Alamitos, 2003), p. 25.

[4] F. Chung, L. Lu, and V. Vu, Proc. Natl. Acad. Sci. U.S.A. **100,** 6313 (2003).

[5] S. N. Dorogovtsev, A. V. Goltsev, J. F. F. Mendes, A. N. Samukhin, Phys. Rev. E **68,** 046109 (2003).

[6] C. Castellano and R. Pastor-Satorras, Phys. Rev. Lett. **105,** 218701 (2010).

[7] S. Gómez, A. Arenas, J. Borge-Holthoefer, S. Meloni, and Y. Moreno, Europhys. Lett. **89,** 38009 (2010).

[8] B. A. Prakash, D. Chakrabarti, M. Faloutsos, N. Valler, and C. Faloutsos, arXiv:1004.0060.

[9] C. Castellano and R. Pastor-Satorras, Sci. Rep. **2,** 371 (2012).

[10] P. Moretti, S. Liu, A. Baronchelli, and R. Pastor-Satorras, Eur. Phys. J. B **85,** 88 (2012).

[11] M. Kitsak, L. K. Gallos, S. Havlin, F. Liljeros, L. Muchnik, H. E. Stanley, and H. A. Makse, Nature Phys. **6,** 888 (2010).

[12] H. Minc, *Nonnegative Matrices* (Wiley-Interscience, New York, 1988).

[13] P. Van Mieghem, Europhys. Lett. **97,** 48004 (2012).

[14] W. W. Zachary, J. Anthropol. Res. **33,** 452 (1977).

[15] M. E. J. Newman, Proc. Natl. Acad. Sci. U.S.A. **98,** 404 (2001).

[16] M. E. J. Newman, Phys. Rev. Lett. **89,** 208701 (2002).

[17] S. N. Dorogovtsev, A. L. Ferreira, A. V. Goltsev, and J. F. F. Mendes, Phys. Rev. E **81,** 031135 (2010).

[18] K.-I. Goh, B. Kahng, and D. Kim, Phys. Rev. Lett. **87,** 278701 (2001).

[19] D.-H. Kim and A. E. Motter, Phys. Rev. Lett. **98,** 248701 (2007).

[20] D. J. Watts and S. H. Strogatz, Nature (London) **393,** 440 (1998).

[21] J. A. Almendral, J. G. Oliveira, L. López, M. A. F. Sanjuán, and J. F. F. Mendes, New J. Phys. **9,** 183 (2007).

[22] CAIDA's router-level topology measurements, http://www.caida.org/tools/measurements/skitter/router_topology/.